Prediction of undrained shear strength characteristics of compacted residual soils

Conference Paper *in* AIP Conference Proceedings · January 2023

DOI: 10.1063/5.0161126

Ukkurthi Venkata Ratnam
Malla Reddy Engineering College

K. Nagendra Prasad
Sri Venkateswara University

Dr J Selwyn babu
Malla Reddy Engineering College

RESEARCH ARTICLE | SEPTEMBER 05 2023

Prediction of undrained shear strength characteristics of compacted residual soils

Venkata Rathnam Ukkurthi; K. Nagendra Prasad; B. Sudarshan Reddy; J. Selwyn Babu

AIP Conference Proceedings 2754, 040003 (2023)
https://doi.org/10.1063/5.0161126

Prediction of Undrained Shear Strength Characteristics of Compacted Residual Soils

Venkata Rathnam Ukkurthi [1, a)] K Nagendra Prasad [2], B. Sudarshan Reddy [1] and J. Selwyn Babu [1]

Author Affiliations
[1] *Department of Civil Engineering, Malla Reddy Engineering College (A), Secunderabad-500100, Telangana, India.*
[2] *Department of Civil Engineering, SVU College of Engineering, SV University Thirupathi, A.P., India*

Author Emails
[a)] Corresponding author: ratnam108@gmail.com

Abstract. The undrained shear strength is critical in the design of foundations as well as the building of other geotechnical constructions such as pavements, backfill material, and embankments. The undrained shear strength represents conservative values of shear strength parameters and in the majority practical cases the undrained shear strength determines the stability aspects of design. The aim of this paper is to understand the effect of intermediate principal stress on undrained strength parameters in relation to Mohr's strength theory wherein the effect of intermediate principal stress is not incorporated. The shear strength behaviour of compacted soils is analysed by considering failure states of the sol both from Mohr's Theory and Critical State Concepts. It is observed that the strength behaviour of compacted soils is different from the behaviour of normally consolidated soils in the sense that cohesion intercept is noticed on q-p plane as well as on τ-s plane. The shear strength parameters are correlated to each other as also with modified plasticity index to propose a framework for analysing the strength behaviour. The data of six different soil samples are used for proposing the phenomenological model and the data of two other samples is used for the purpose of prediction. According to the results of the investigation, the suggested framework can be used to evaluate the shear strength of compacted residual soils.

INTRODUCTION

Compaction of soils are extensively used in road construction, earth fills, dams and other infrastructure projects. The properties of concern to an engineer are shear strength and compressibility. The compacted soils come under the ambit of unsaturated soils as the soils compacted at the optimum moisture contents would have saturation ranging from 85% to 95%. The compacted soils are known to exhibit additional resistance owing to menisci caused due to unsaturation and the interlocking imparted due to applied stress as compared to normally consolidated soils. It is widely known that the data on unsaturated soils is relatively less documented as compared to normally consolidated soils.

The structural strength is first and foremost a function of shear strength. Soil failure usually occurs in the form of "shearing" along internal surface within the soil, shear strength is a soils ability to resist sliding along internal surfaces within the soil mass. The strength of clayey soil is influenced by compaction energy, optimum moisture content, dry density, percentage of fines, degree of saturation and consistency limits, cohesion between the soil particles and frictional resistance between the particles. According to Mohr's theory, a soil mass will fail when the shearing stress on the failure plane, which is a definite function of the normal stress acting on that plane, is greater than the shear resistance of the soils i. e. S = F(σ) The shearing strength of a soil is represented by the following Coulomb's equation.

$$S = c + \sigma tan\emptyset$$

International Conference on Materials, Processing & Characterization
AIP Conf. Proc. 2754, 040003-1–040003-12; https://doi.org/10.1063/5.0161126
Published by AIP Publishing. 978-0-7354-4634-2/$30.00

Where S = shear stress at failure,
c = cohesion
σ = Normal stress and
 = Angle of internal friction.

The angle of internal friction depends upon dry density, particle size distribution, shape of particles, surface texture, and water content. Cohesion depends upon size of clayey particles, types of clay minerals, valence bond between particles, water content, and proportion of the clay (Rajeev Jain et al. 2010). As a result, geotechnical engineers are keen to know about the shear strength behaviour of both natural and compacted residual soils, which are frequently referred to as problematic soils in the literature (Rahardjo et al., 1995; Pereira et al., 2000; Toll and Ong, 2003; Rahardjo et al., 2004; Futai and Almeida, 2005; Matsushi and Matsukura, 2006; Kayadelen et al., 2007).

BACKGROUND INFORMATION

While soil mechanics has been established mostly on the basis of pure sand or pure clay test findings, the soils encountered in the field are typically mixes of diverse soils. Because the percentage of fine and coarse grains might be unlimited, it is exceedingly difficult to define the mechanical behaviour of such soil combinations in a few parameters, (Kim et al. 2018).

Shear strength is the most essential engineering feature of soil and is responsible for its capacity to bear applied loads. Shear strength is measured directly in the field or in a laboratory, but several empirical correlations have been constructed to predict shear strength from fundamental and index soil parameters. Direct measurements are expensive, time-consuming, and not always appropriate, which is why these correlations are used. (Daoud et al. 2016). Nagendra Prasad (2013) used a hyperbolic technique to create a basic constitutive relationship utilising test findings from five distinct types of soils in a properly designed experimental investigation. To capture the strain softening behaviour of residual soils, a combination of stress ratio and mean primary stress is found. Soil, unlike other engineering materials, resists applied loads by friction and particle cohesion, which is known as shear strength. Soil shearing resistance is primarily determined by soil composition, stress history, strain, strain rate, void ratio, cohesion, and particle friction (Mitchell and Soga 2005). A functional form that takes into account all of these elements is too complicated, thus numerous simplifications were developed to measure the soil's shear strength. The Mohr–Coulomb equation, which reduces soil shear strength to rely only on cohesion, internal friction angle, and confining stress, is the most extensively used functional form of shear strength (Bowles 1996). The shear strength parameters, soil cohesion and internal friction angle, can be determined immediately in the field or in the laboratory. Precise measurement of shear strength parameters is expensive, time-consuming, and not always appropriate (Phoon and Kulhawy 1999). This demands the creation and use of empirical correlations. The development of shear strength correlations began in the 1940s, and new correlations are constantly being generated currently. The majority of cohesive soil correlations are based on soil flexibility since cohesion is primarily determined by clay mineral types, clay particle size, clay percentage, and particle bonding.

MATERIALS AND METHODS

The current experimental research has been meticulously designed in order to provide a framework for analysis and assessment of soil behaviour. The soil samples from eight different locations were brought to laboratory after removing the top filled up soil. The soils are brought to the laboratory for further processing. The soil samples were air dried and sieved through 20mm sieve and the fraction passing through the 20mm sieve has been used for conducting the experimental study. The experimental program involves determination of the following aspects.

- Basic Soil properties [classification tests]
- Mechanical properties of soils [strength characteristics]

All tests are carried out in accordance with the applicable rules outlined in the Bureau of Indian Standards, as shown in Table 1. Table 2 displays the characteristics of the soils.

Table 1: Tests conducted

Test Conducted	IS Code of Practice
Grain size Distribution	IS 2720-4:1985
Liquid Limit	IS 2720-5:1985
Plastic Limit	
Specific Gravity	IS : 2720 (Part III/Sec 1-1980
Free Swell Index	IS 2720-40:1977
Maximum Dry Density	IS 2720-7:1980
Optimum Moisture Content	
Triaxial Shear Compression	IS: 2720 (Part. XI) 1993
Unconfined Compressive Strength	IS: 2720 (Part. X) 1991

The soil samples designation and details of locations are as follows:

- S1 (Renigunta)
- S2 (Chipllivage, Madanapalle)
- S3 (Yedugundlapadu, Ongole)
- S4 (Mungamur Canal Road, Ongole)
- S5 (Tirupati, Bypass)
- S6 (Tiruchanur, Tirupati)
- S7 (Annasampalli Road, Renigunta)
- S8 (YSR Kadapa).

Table 2 depicts the basic properties of eight soils. The grain size distribution obtained from dry sieve analysis is integrated with hydrometer analysis and the particle size distribution curves thus obtained are presented in Figure 1. It may be seen that grain sizes and Atterberg limits represent wide spectrum in terms of soil classification (IS: 1498-1970) ranging from Clayey Sand (SC) to Clay with high Compressibility (CH).

Table 2: Basic Properties of soils

S.No	Properties	S1	S2	S3	S4	S5	S6	S7	S8
1	**Specific Gravity**	2.74	2.63	2.56	2.76	2.73	2.65	2.65	2.5
2	Gravel (%)	9.20	1.20	3	1.16	1.20	4.20	2.22	6.41
	Sand (%)	47.00	24.00	19	63.47	62.10	47.40	47.17	14.90
	Silt (%)	37.42	34.31	21.49	20.46	24.49	30.75	32.26	65.91
	Clay (%)	6.38	40.49	56.51	14.91	12.21	17.65	18.34	12.78
	% Passing 425 ❑	66.2	86.74	93.51	52.25	58	68	85.43	82.62
3	Liquid Limit (%)	62.00	41.50	51.00	32.50	81.50	65.50	60.00	55.00
	Plastic Limit (%)	27.00	21.00	19.00	24.60	21.00	19.00	16.27	17.00
	Plasticity Index (%)	35.00	20.50	32.00	8.0	60.50	46.50	43.73	38.00
4	**IS Classification 1498-1970)**	**SC**	**CI**	**CH**	**SM**	**SC**	**SC**	**SC**	**CH**
5	**Free Swell Index,%**	110	108	105	60	182	160	135	110
6	**Maximum Dry Density,kN/m^3**	19.00	18.12	17.90	19.22	19.50	18.80	18.75	18.10
7	**Optimum Moisture content,%**	15.00	17.00	16.50	14.50	14.00	14.50	15.50	16.90

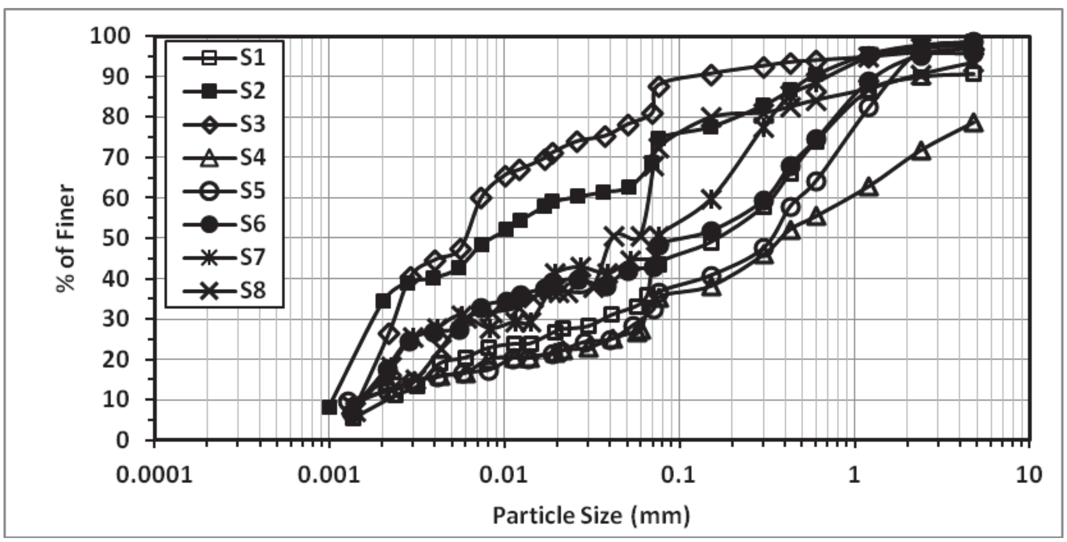

Figure 1: Grain Size Distribution Curves

ANALYSIS OF TEST RESULTS

The present study considers eight soil samples consisting of inherent variation interms of grain size distribution and consistency limits. Unconsolidated undrained tests, a typical method of assessing soil shear strength, were performed on these samples to be cautious. Despite the fact that cell pressure is often supplied to the specimen during testing, the sample is not allowed to consolidate, i.e. the drainage line is retained closed under cell pressure before the shear phase of the test is done. (Atkinson and Bransby, 1978).

The samples have been prepared at respective optimum moisture content using standard Proctor's compaction energy to ensure uniform sample preparation. The samples of 38 mm diameter and 76 mm height have been extracted for carrying out triaxial compression tests. Confining pressure of 100 kPa and 200 kPa has been applied to observe the deviatoric stress at failure for all the samples investigated.. In addition unconfined compression tests are also conducted for the specimens prepared under similar conditions as those of triaxial compression tests.

It may be seen from tests that shear behaviour is characterised by peak values of deviatoric stress followed by fall in the stress-strain behaviour. Further, for any given stress diagram, the deformation experienced by the soil is found to be higher for the unconfined compression tests. The same feature is noticed with respect to all eight samples. Based on the experimental results obtained, Mohr's circles have been drawn to fit the experimental data in order to determine the cohesion intercept and angle of internal friction. These Mohr's circles are shown in Figures 1 to 8.

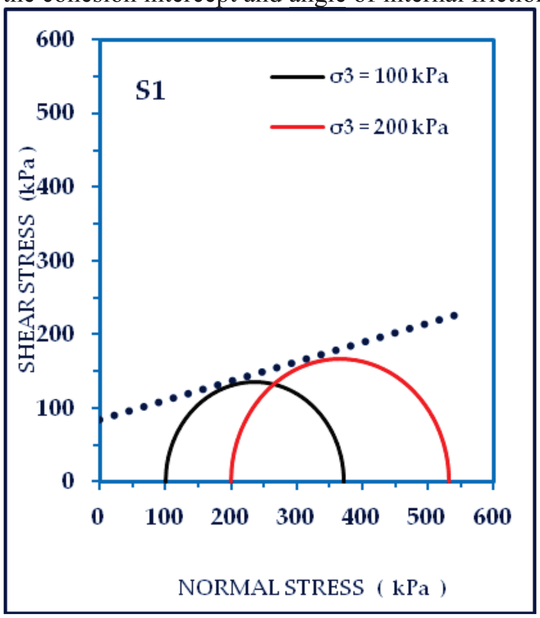

Figure: 2 Mohr's circles for sample 1

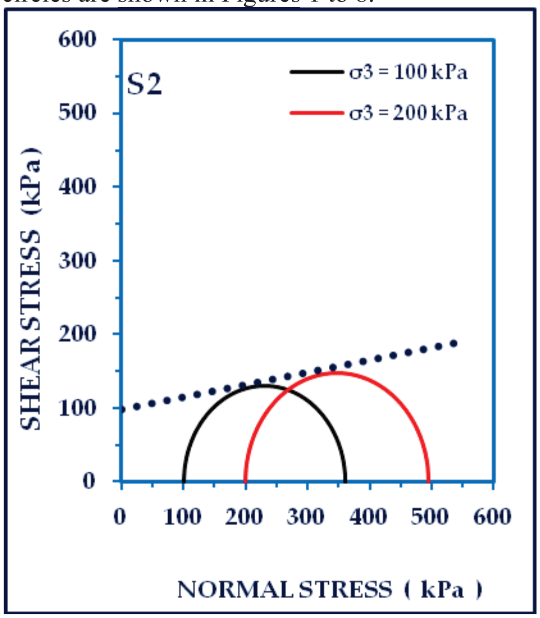

Figure: 3 Mohr's circles for sample 2

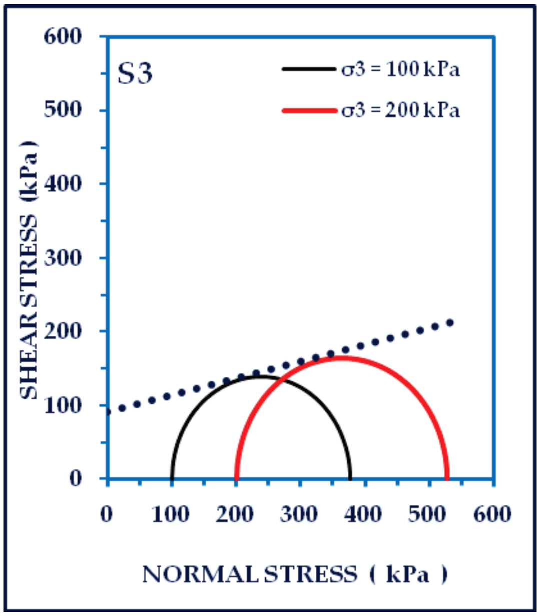

Figure:4 Mohr's circles for sample 3

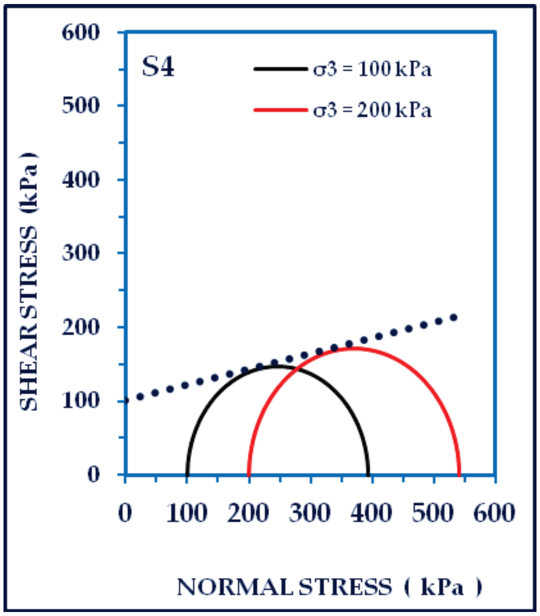

Figure:5 Mohr's circles for sample 4

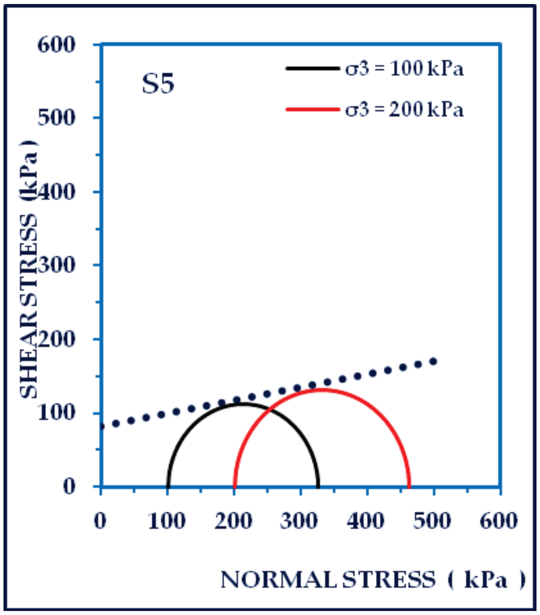

Figure: 6 Mohr's circles for sample 5

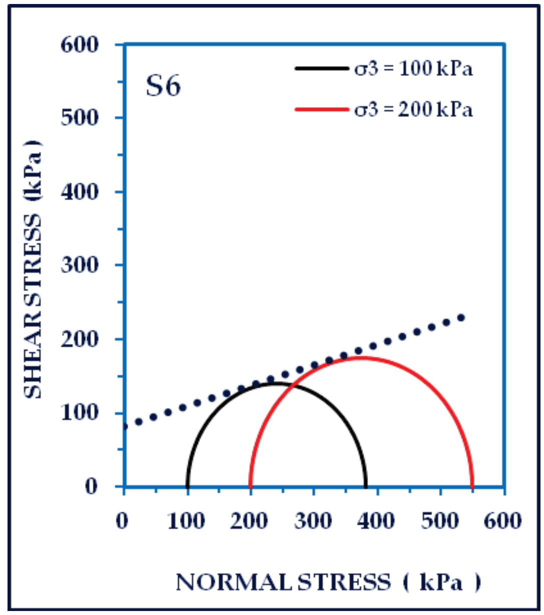

Figure: 7 Mohr's circles for sample 6

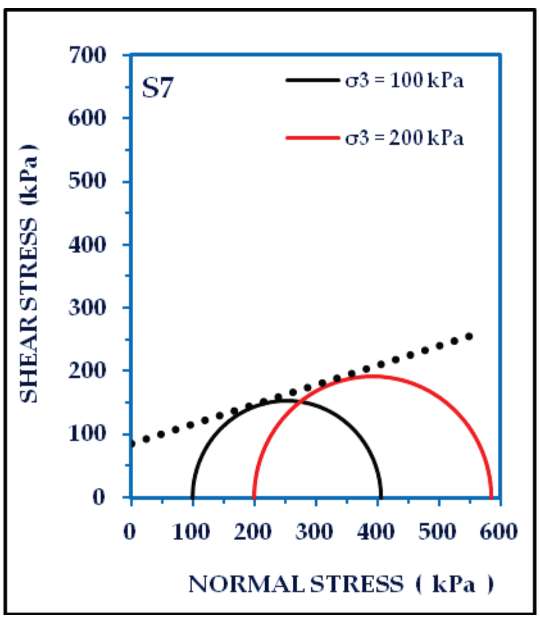

Figure:8 Mohr's circles for sample7

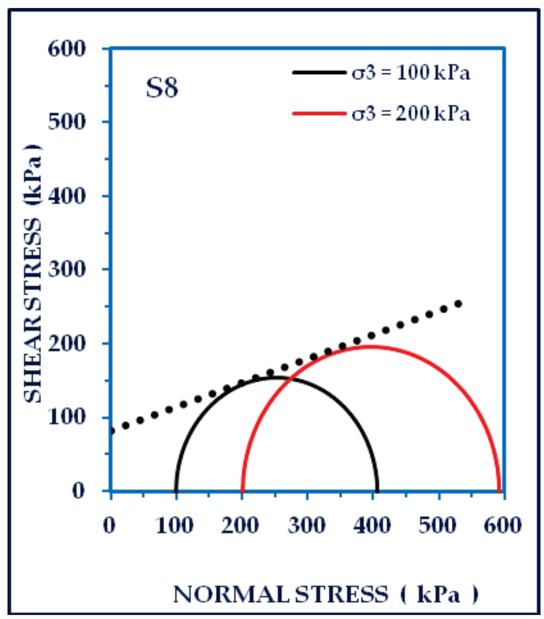

Figure: 9 Mohr's circles for sample 8

The tangents drawn to be Mohr's circles have initiated the relationship between shear strength and shear parameters c and ϕ with the following relationship.

$$r_f = \boldsymbol{c} + \boldsymbol{\sigma} \, \boldsymbol{tan}\emptyset \qquad \textit{Equation} \quad 1$$

Where S = shear stress at failure,
c = cohesion
σ = Normal stress and
ϕ = Angle of internal friction.

The above expression obtained for all the eight samples for compacted state at respective optimum moisture contents indicates evaluation of cohesion intercept and angle of internal friction which is not the case for the normally consolidated soils. This turns out that the behaviour of compacted soils is different as compared to normally consolidated soils. The cohesion intercept may be ascribed to partial saturation and/or to interlocking effect imparts on account of compactive energy. The above expression does not incorporate the effect of intermediate principle stress. Accordingly, an attempt has been made to re-plot the experimental data on the stress parameters shown as follows:

$$p = \frac{\sigma_1 + 2\sigma_3}{3} \qquad \textit{Equation} \quad 2$$

$$q = \sigma_1 - \sigma_3 \qquad \textit{Equation} \quad 3$$

Where, p = Mean principal stress in kPa
q =Deviatoric stress in kPa
σ_1 =axial stress on a cylindrical sample
σ_3 =radial stress on a cylindrical sample

It may be seen from the above chosen shear parameters, the confining pressure on which the shear strength dependence, involves the effect of intermediate principle stress also. Further, the stress paths are traced on q'-p platform to interpret the data on critical state frame work.
Since, in the undrained test, pore water pressures are not measured, the total stress parameters are used for plotting the stress paths. The experimental data plotted on q-p platform may be seen from Figures 9 to 16.

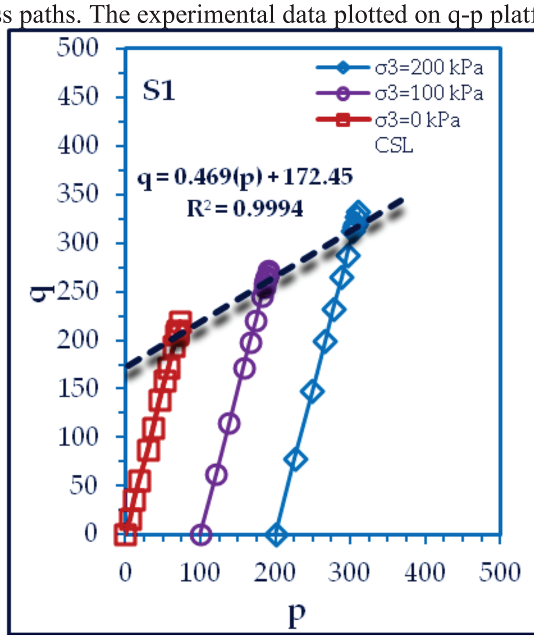

Figure: 10 stress paths for sample 1

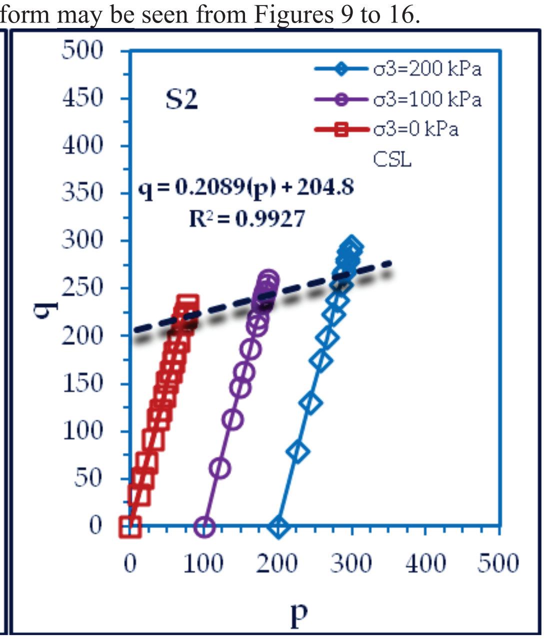

Figure: 11 stress paths for sample 2

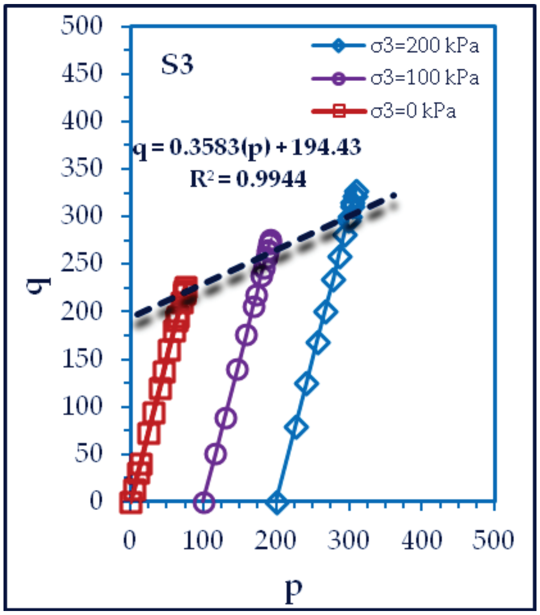

Figure: 12 stress paths for sample 3

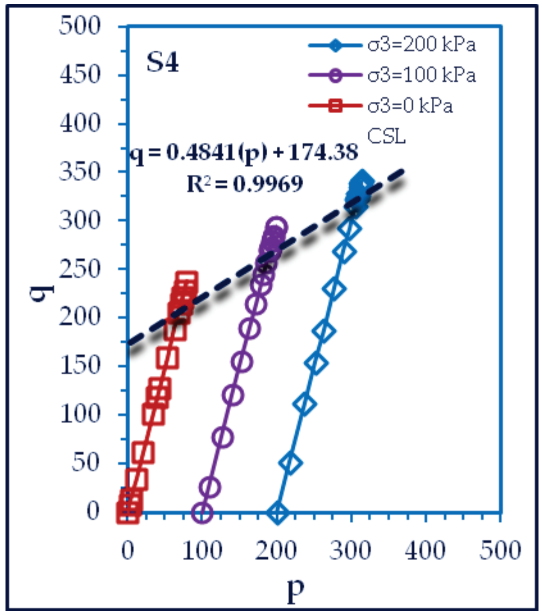

Figure:13 stress paths for sample 4

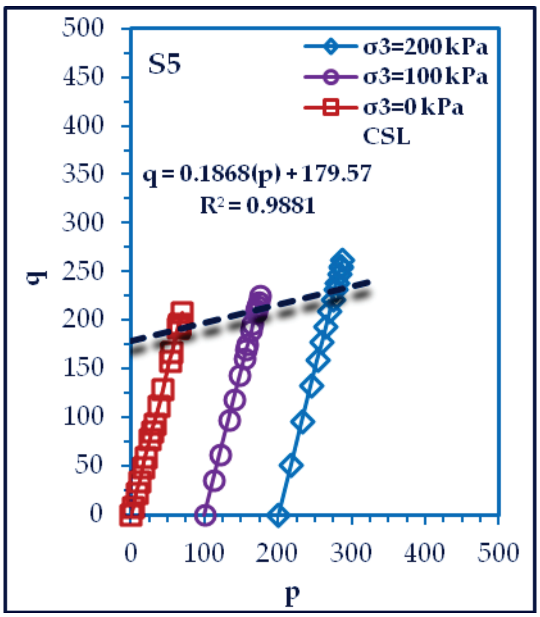

Figure: 14 stress paths for sample 5

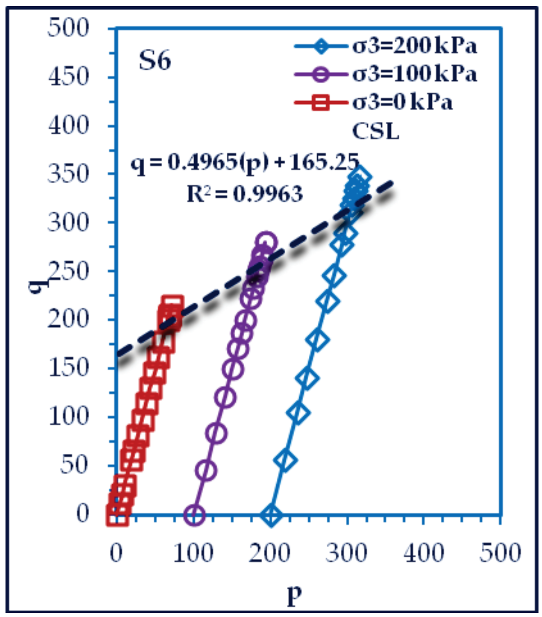

Figure: 15 stress paths for sample 6

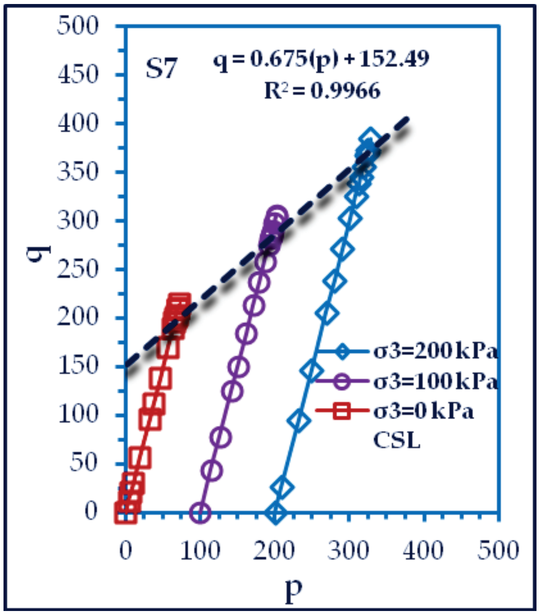

Figure: 16 stress paths for sample 7

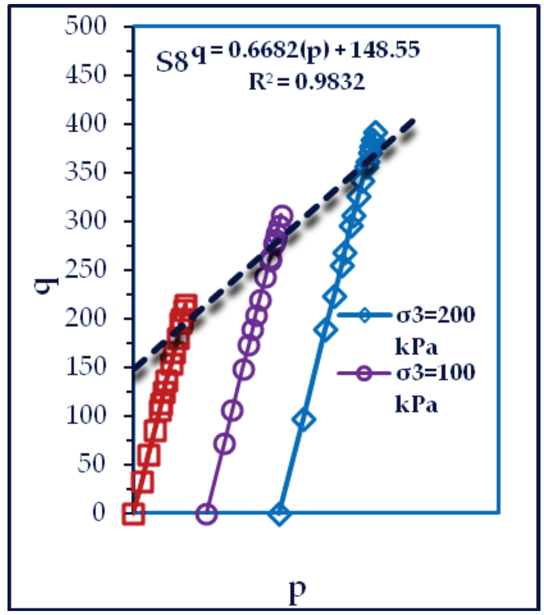

Figure: 17 stress paths for sample 8

RESULTS AND DISCUSSIONS

It may be noticed from the figures (9 to 16) that the critical state, the state where there is no change in stress with strain fall on same line, for all the eight samples as given by the following expression:

$$q = \mu + Mp \qquad \textit{Equation 4}$$

Where, μ = Intercept found on deviatoric stress axis

M = Friction coefficient

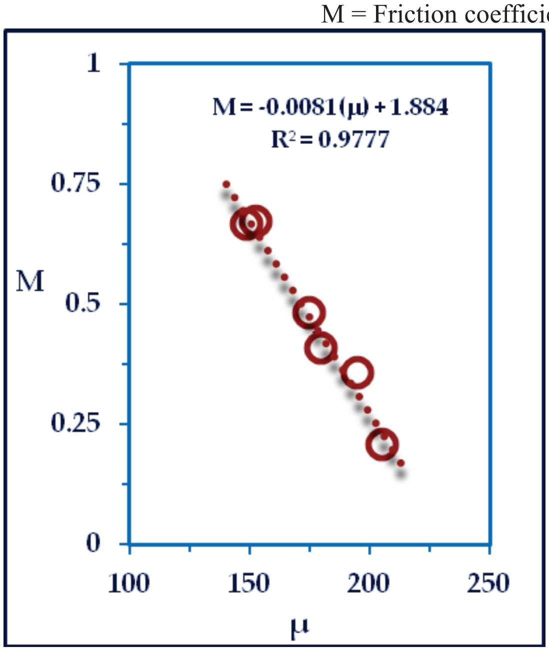

Figure: 18 Friction coefficient M and Cohesion intercept

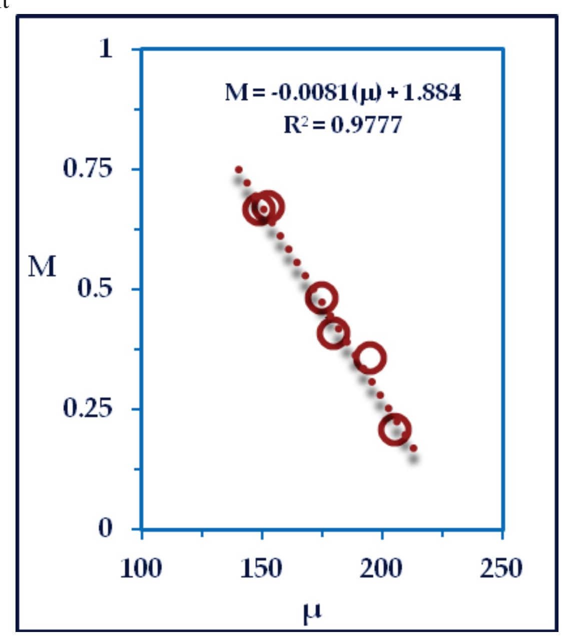

Figure: 19 Cohesion intercept and Modified plasticity index Imp

As explained before, the cohesion intercept depends upon degree of compaction and degree of saturation. The values of friction coefficient M and $\boldsymbol{\mu}$ cohesion intercept are plotted to find out the possible relationship between these two values the relationship obtained by using the data of six soil samples is shown in figure 17. The following relationship is obtained:

$$\boldsymbol{M = 1.884 - 0.0081(\mu)} \text{ with } R^2 = 0.9777 \qquad \textit{Equation 5}$$

In order to establish the above critical state parameters, an attempt has been made to find out normalised values of the cohesion intercept with basic index properties. The above exercise has led to the expressions with a correlation coefficient of 0.967 has been obtained with Modified plasticity index I_{mp} as shown in figure 18. The expression is given by

$$\mu/\boldsymbol{\sigma y} = \mathbf{2.5921} + \mathbf{0.0435}\ (\text{Imp}) \text{ with R2 } = 0.967 \qquad \text{Equation 6}$$

Where, σ_y = yield stress in one dimensional compression
I_{mp} = modified plasticity index

From equation 5 and 6 it is clear that the values of can be obtained from equation 6 and the value M is obtained from equation 5. From the aforementioned discussion it is evident that the failure conditions of samples tested under different stress path conditions can be predicted on the values of M and $\boldsymbol{\mu}$ are evaluated from expressions 5 and 6. Accordingly, the data of the other two samples have been predicted by the following the procedure proposed. The results of the predictions are presented in Table 3.

Table: 3 Prediction of q-p at confinement pressure 0 kPa

Sample No	INPUT			Experimental Results				Predicted Results		Percentage Difference %	
	Imp %	$\boldsymbol{\mu}$ kPa	P_0 kPa	$\boldsymbol{\mu}$ kPa	M	p kPa	q kPa	p	q	p	q
1	66.20	46	0	174.49	0.47	68.99	206.96	68.45	205.35	0.78	0.78
8	82.62	43	0	163.31	0.56	66.96	200.89	66.67	200.00	0.44	0.44

Table: 4 Prediction of q-p at confinement pressure 100 kPa

ample No	INPUT			Experimental Results				Predicted Results		% Difference	
	Imp %	y kPa	P kPa	y kPa	M	p kPa	q kPa	p	q	p	q
1	27.54	46	100	174.34	0.471	187.6	262.86	186.0	258.12	0.85	1.84
8	27.64	43	100	163.16	0.562	190.0	270.01	186.7	260.37	1.72	3.70

Table: 5 prediction of q-p at confinement pressure 200 kPa

Sample No	INPUT			Experimental Results				Predicted Results		% Difference	
	Imp %	y kPa	P kPa	y kPa	M	p kPa	q kPa	p	q	p	q
1	27.54	46	200	174.34	0.471	306.28	318.85	305.50	316.50	0.26	0.74
8	27.64	43	200	163.16	0.562	313.07	339.21	323.61	370.84	-3.26	-8.53

From the above Tables 3 to 5, it clearly indicates that the percentage difference between predicted and experimental values is within the range of about 9% reflecting that the procedure proposed predicts the failure conditions by closely.

Effect of intermediate Principle stress

The interpretation of experimental results using Mohr's Circle concept based on the expression, $\sigma_1 = \sigma_3 \tan^2\alpha + 2c \tan\alpha$ has yielded the values of cohesion intercept, c and friction coefficient, M are indicated in table 6.

Table: 6 Experimental Results (Mohr's Circle concept)

Sample No	Cohesion intercept,µ kPa	friction coefficient, M
1	166.430	0.486
2	196.569	0.254
3	203.371	0.408
4	201.789	0.447
5	171.051	0.217
6	152.116	0.548
7	152.679	0.689
8	137.830	0.814

For µ and M refer appendix 1

The interpretations of experimental data based on critical state framework have yielded the values of cohesion intercept and friction coefficient M which are shown in table 7.

Table: 7 Predicted Results (critical state framework)

Sample No	Cohesion intercept, µ kPa	friction coefficient, M
1	172.450	0.469
2	204.800	0.209
3	194.430	0.358
4	174.380	0.484
5	179.570	0.187
6	165.250	0.497
7	152.490	0.675
8	148.550	0.668

The comparison between the above two tables in respect of respective share parameters indicates that there is a noticeable effect of intermediate principle stress as the values of µ and M with the value of M as the decrease where µ is the value of cohesion intercept on the increase. This turns out the intermediate principle stress enhance the confinement and results in increase in values of cohesion intercept in relation to frictional coefficient.

CONCLUSIONS

Based on detailed experimental investigation and analysis of test results the following concluding remarks may be made.

- The strength behaviour of compacted soils is different from the behaviour of normally consolidated soils
- The shear strength behaviour of compacted soils comprise of cohesion intercept and friction coefficient
- The cohesion intercept may arise from unsaturation leading to formation of capillary menisci imparting additional resistance and due to interlocking arising from dense state of packing.
- The critical state line for compacted soils is of the form : $q = Mp + \mu$ in terms of q, p parameters and $t = s + c\ tan\emptyset$ interms of two dimensional parameters.
- The effect of intermediate principal stress is to increase the cohesion intercept by about 10% while the friction coefficient fairly remains unaffected.

REFERENCES

1. Bowles, J.E. (1996). *Foundation analysis and design*. New Delhi: Mcgraw-Hill Education (India) Private Limited.
2. Code, I.S., IS 1498–1970. Classification and identification of soils for general engineering purposes (first revision).
3. Code, I.S., IS 2720 (Part–40)–1977. Determination of free swell index of soils.
4. Daoud, W., Kasama, K., Saleh, N. and Negm, A. (2016). Ranking and transformation error assessment of shear strength parameters correlations. *International Journal of Geo-Engineering*, 7(1).
5. Futai, M.M. and Almeida, M.S.S. (2005). An experimental investigation of the mechanical behaviour of an unsaturated gneiss residual soil. *Géotechnique*, 55(3), pp.201–213.
6. James Kenneth Mitchell and Kenichi Soga (2005). *Fundamentals of soil behavior*. Hoboken, Nj: John Wiley & Sons.
7. John Herbert Atkinson and Bransby, P.L. (2012). *The mechanics of soils: an introduction to critical state soil mechanics*. Delhi: Indo American Books.
8. Karim, M.E. and Alam, Md.J. (2017). Effect of nonplastic silt content on undrained shear strength of sand–silt mixtures. *International Journal of Geo-Engineering*, 8(1).
9. Kayadelen, C., Tekinsoy, M.A. and Taşkıran, T. (2007). Influence of matric suction on shear strength behavior of a residual clayey soil. *Environmental Geology*, 53(4), pp.891–901.
10. Kim, D., Nam, B.H. and Youn, H. (2018). Effect of clay content on the shear strength of clay–sand mixture. *International Journal of Geo-Engineering*, 9(1).
11. K-K, P., FH, K. and MD, G. (1995). *Reliability-based Design for Transmission Line Structure foundations.* Thesis.
12. Matsushi, Y. and Matsukura, Y. (2006). Cohesion of unsaturated residual soils as a function of volumetric water content. *Bulletin of Engineering Geology and the Environment*, 65(4), pp.449–455.
13. Nagaraj, H.B. (2016). Influence of gradation and proportion of sand on stress–strain behavior of clay–sand mixtures. *International Journal of Geo-Engineering*, 7(1).
14. Pereira, J.H.F. and Fredlund, D.G. (2000). Volume Change Behavior of Collapsible Compacted Gneiss Soil. *Journal of Geotechnical and Geoenvironmental Engineering*, 126(10), pp.907–916.
15. Prasad, K. and Sulochana, N. (2013). Hyperbolic Constitutive Model for Tropical Residual Soils. *International Journal of Civil Engineering and Technology*, 4(3), pp.121–133.
16. Rahardjo, H., Heng, O.B. and Choon, L.E. (2004). Shear strength of a compacted residual soil from consolidated drained and constant water content triaxial tests. *Canadian Geotechnical Journal*, 41(3), pp.421–436.
17. Rahardjo, H., Lim, T.T., Chang, M.F. and Fredlund, D.G. (1995). Shear-strength characteristics of a residual soil. *Canadian Geotechnical Journal*, 32(1), pp.60–77.
18. Standard, I., 2720 (Part 7)-1980. Determination of Water Content, Dry Density relation of Soil using Light Compaction.
19. Standard, I., IS: 2720 (Part 11)–(1993). Determination of the shear strength parameters of a specimen tested in unconsolidated undrained triaxial compression without the measurement of pore water pressure.
20. Standard, I.I., 1991. 2720 (Part 10): Method of test for soils: Determination of unconfined compressive strength. Bureau of Indian Standards, Delhi, India.
21. Standard-IS, I., 2720 (Part 4)–(1985) Methods of test for soils, determination of grain size analysis of soil. New Delhi, India.
22. Standard-IS, I., 2720 (Part 5) 1985 Methods of test for soils, determination of liquid and plastic limit of soils. New Delhi, India.
23. Standard-IS, I., IS 2720 (Part 3) 1980. Methods of test for soils, determination of specific gravity, fine, medium and coarse grained soils, New Delhi.
24. Toll, D.G. and Ong, B.H. (2003). Critical-state parameters for an unsaturated residual sandy clay. *Géotechnique*, 53(1), pp.93–103.